Weak ferromagnetic ordering in Ca doped polycrystalline BiFeO3

B. Ramachandran, A. Dixit, R. Naik, G. Lawes, and M. S. Ramachandra Rao

Related Articles

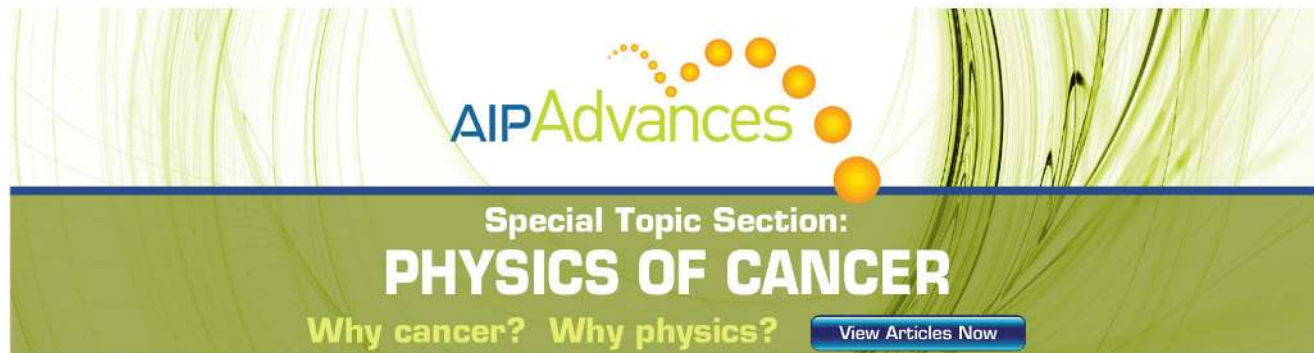## Additional information on J. Appl. Phys.

Journal Homepage: http://jap.aip.org/

Journal Information: http://jap.aip.org/about/about_the_journal

Top downloads: http://jap.aip.org/features/most_downloaded

Information for Authors: http://jap.aip.org/authors

Weak ferromagnetic ordering in Ca doped polycrystalline BiFeO$_3$

B. Ramachandran,[1,a)] A. Dixit,[2] R. Naik,[2] G. Lawes,[2] and M. S. Ramachandra Rao[1]

[1]*Department of Physics, Nano Functional Materials Technology Centre and Materials Science Research Centre, Indian Institute of Technology Madras, Chennai, 600036, Tamil Nadu, India*
[2]*Department of Physics and Astronomy, Wayne State University, Detroit, Michigan, 48201, USA*

Structural and magnetic properties of polycrystalline BiFeO$_3$, Bi$_{0.9}$Ca$_{0.1}$FeO$_{2.95}$, Bi$_{0.9}$Ba$_{0.05}$Ca$_{0.05}$FeO$_{2.95}$, and Bi$_{0.9}$Ba$_{0.1}$FeO$_{2.95}$ ceramic samples were studied to establish the effects of doping in BiFeO$_3$ on the magnetic property. X-ray diffraction data of the undoped and doped BiFeO$_3$ samples were refined to a rhombohedral structure with space group *R3c*. X-ray photoelectron spectroscopy study showed the formation of a single-phase in both the undoped and doped BiFeO$_3$ ceramics with Fe in the 3+ valence state. Ca doped and Ba-Ca co-doped BiFeO$_3$ ceramic samples show weak ferromagnetic ordering at room temperature. This observation makes Ca doped and Ba-Ca co-doped BiFeO$_3$ samples an interesting material system for magnetoelectric coupling studies. © *2012 American Institute of Physics*. [doi:10.1063/1.3678449]

I. INTRODUCTION

The current interest in multiferroic materials stems from the fact that the ferromagnetic and ferroelectric order parameter coupling in terms modulating electrical polarization with a magnetic field and magnetization with an electric field can produce new technologies.[1–6] In addition, magnetic control of the dielectric permittivity in multiferroic oxide materials can be exploited to create new kinds of high frequency filters and wireless sensors.[6–9] One of the best known multiferroic materials is BiFeO$_3$ in which the ferroelectric and antiferromagnetic orders appear near 1100 K and 640 K, respectively.[9] Its room temperature crystal structure is described by the rhombohedral space group *R3c*, which is non-centrosymmetric. However, magnetoelectric interactions in bulk samples of pure BiFeO$_3$ are weak because of the underlying antiferromagnetic *G*-type structure that is modulated by a cycloid with a large period of 620 Å.[10] The saturation polarization in this material can routinely reach as much as 60 μC/cm^2 in suitably prepared thin films,[11] although it is generally much smaller in bulk samples, plausibly due to an increased leakage current.[12,13] The maximum polarization values are now found to reach ∼90 μC/cm^2 along the [111] direction of the pseudo-cubic perovskite unit cell, consistent with first-principles calculations.[14] The large difference between the thin-film and bulk values, initially attributed to epitaxial strain,[11] could also result from leakage effects in crystals caused by defect chemistry or the existence of second phases or mechanical constraints in granular bulk ceramics. However, ferro- or ferrimagnetism instead of antiferromagnetism together with an enhanced polarization is highly preferable for low-field practical applications. Enhancements in the magnetization and ferroelectric polarization were reported in the A-site doped Bi$_{0.9-x}$Tb$_x$La$_{0.1}$FeO$_3$ systems where Tb and La

are isovalent to Bi^{3+} ions, and also in Bi$_{1-x}$Nd$_x$FeO$_3$.[15,16] Interestingly, divalent cation (A) substituted Bi$_{0.7}$A$_{0.3}$FeO$_{2.95}$ (A = Ca, Sr, Pb, and Ba) exhibits enhanced magnetization.[17] The improved magnetic property was also observed in 5% alkaline earth metals (Ba, Sr, and Ca) substituted BiFeO$_3$ nanoparticles.[18] Recently, Yang *et al.* showed the presence of a ferroelectric-paraelectric boundary in divalent-ion-calcium doped multiferroic BiFeO$_3$ films substituted with Ca at an atomic fraction of ∼0.125.[19] In all these reports, one can find that the doping concentration level is high (x ≥ 0.1); this eventually leads to structural distortion. Moreover, the synthesis of single-phase and highly dense undoped and doped BiFeO$_3$ ceramic samples is challenging because of the highly volatile nature of Bi during the sintering process. In the present work, our main aim is to prepare single-phase undoped and Ba, Ca

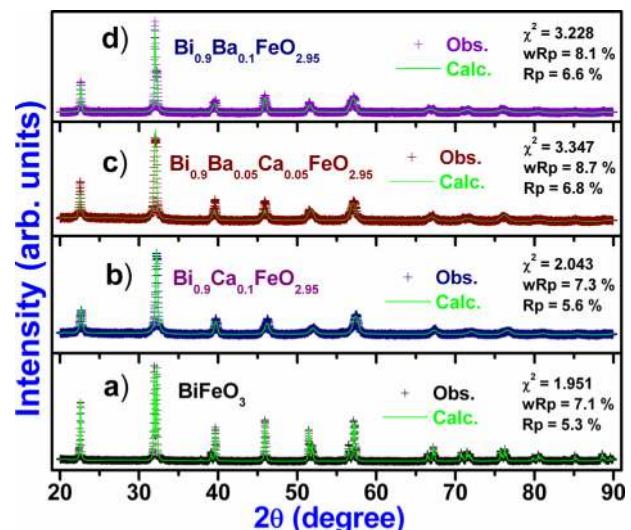FIG. 1. (Color online) Rietveld refined XRD patterns of (a) BiFeO$_3$, (b) Bi$_{0.9}$Ca$_{0.1}$FeO$_{2.95}$, (c) Bi$_{0.9}$Ba$_{0.05}$Ca$_{0.05}$FeO$_{2.95}$, and (d) Bi$_{0.9}$Ca$_{0.1}$FeO$_{2.95}$ ceramics sintered at 850 °C for 6 h.

a)Author to whom correspondence should be addressed. Electronic mail: ramchandar@physics.iitm.ac.in.
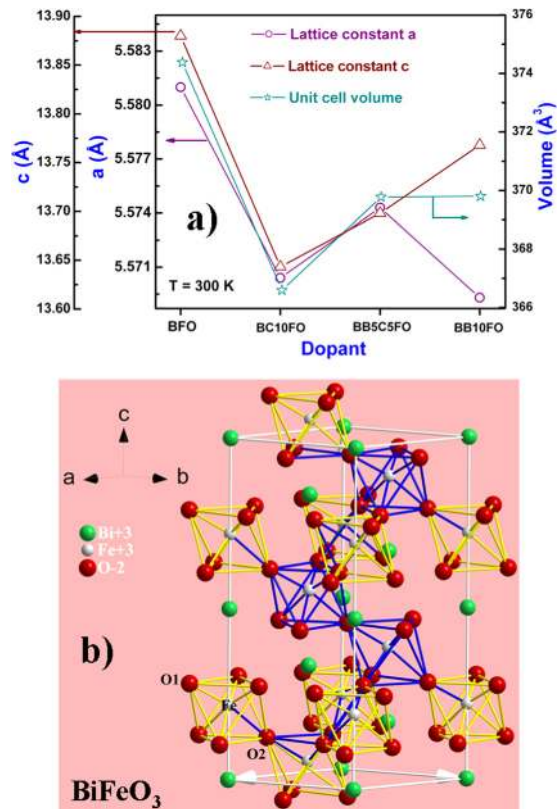
FIG. 2. (Color online) (a) Lattice constants and unit cell volume vs dopant and (b) crystal structure of BiFeO₃. Blue and yellow color bonds represent bonds that are inside and outside of the unit cell in the Fe-O octahedra, respectively.

doped BiFeO$_3$ ceramic samples while maintaining the rhombohedral crystal symmetry to improve their magnetic property. This will help to clarify the fundamental intrinsic properties of bulk BiFeO$_3$.

TABLE I. Bond length and bond angle of Fe1-O-Fe2 bonds of the undoped and doped polycrystalline BiFeO$_3$ samples.

Sample	Bond length (Å)	Bond angle (°)
BiFeO$_3$	Fe-O1 – 1.903	Fe1-O-Fe2 – 157.39
	Fe-O2 – 2.141	
Bi$_{0.9}$Ca$_{0.1}$FeO$_{2.95}$	Fe-O1 – 1.893	Fe1-O-Fe2 – 157.33
	Fe-O2 – 2.124	
Bi$_{0.9}$Ba$_{0.05}$Ca$_{0.05}$FeO$_{2.95}$	Fe-O1 – 1.896	Fe1-O-Fe2 – 157.35
	Fe-O2 – 2.128	
Bi$_{0.9}$Ba$_{0.1}$FeO$_{2.95}$	Fe-O1 – 1.897	Fe1-O-Fe2 – 157.37
	Fe-O2 – 2.131	

II. EXPERIMENTAL DETAILS

We have synthesized calcium and barium doped polycrystalline BiFeO$_3$ ceramic samples through an ethanol mediated sol-gel route.[20] The final sintering process of the undoped and doped BiFeO$_3$ samples was done at 850°C for 6 h. The x-ray diffraction (XRD) data of the BiFeO$_3$ (BFO), Bi$_{0.9}$Ca$_{0.1}$FeO$_{2.95}$ (BC10FO), Bi$_{0.9}$Ba$_{0.05}$Ca$_{0.05}$FeO$_{2.95}$ (BB5C5FO), and Bi$_{0.9}$Ba$_{0.1}$FeO$_{2.95}$ (BB10FO) samples were collected using a PANalytical X'Pert Pro x-ray diffractometer with Cu $K\alpha$ radiation. Morphology and composition analysis of the samples were studied using field emission scanning electron microscope and energy dispersive x-ray spectrum analysis. Elemental analysis of the undoped and doped BiFeO$_3$ samples was carried out using an x-ray photoelectron spectroscopy system from Perkins Elmer. The magnetization data of the undoped and doped BiFeO$_3$ samples were measured using physical property measurement system from Quantum Design.

III. RESULTS AND DISCUSSION

The phase formation of undoped and doped BiFeO$_3$ ceramic samples was confirmed by x-ray diffraction (XRD).
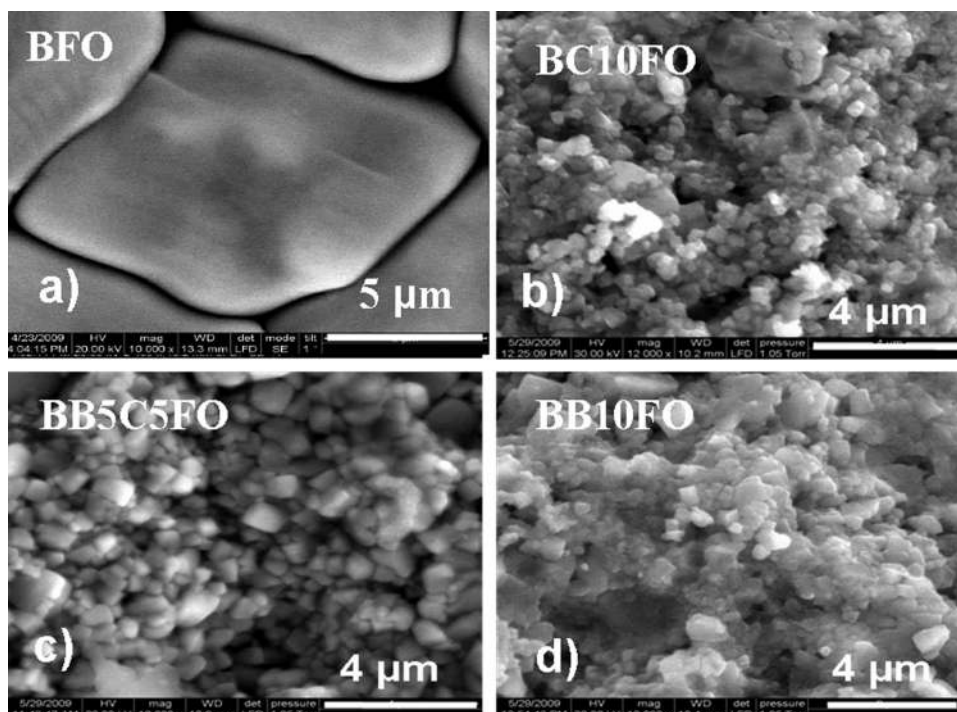

FIG. 3. FESEM images of (a) BFO, (b) BC10FO, (c) BB5C5FO, and (d) BB10FO ceramics.

Crystal structure refinements were carried out using the GEN-ERAL STRUCTURE ANALYSIS SYSTEM (GSAS) software package.[21] Fig. 1 shows the results of the Rietveld refinement of the XRD patterns of undoped and doped BiFeO$_3$ samples sintered at 850°C for 6 h. The refinement was carried out using the rhombohedral crystal symmetry with *R3c* space group in a hexagonal lattice. We obtained good fits for all the samples with good *R* factors, as indicated in each individual plot of Fig. 1. The lattice constants and unit cell volume extracted from these fits were plotted against dopant as shown in Fig. 2(a). The lattice constant and unit cell volume were reduced for all doped samples as compared to those for undoped BiFeO$_3$. The crystal structure of BiFeO$_3$ was drawn using the obtained cell parameters using the DIAMOND software package (Fig. 2(b)). The estimated bond length and bond angle of the Fe1-O-Fe2 bonds in the doped BiFeO$_3$ samples were found to decrease relative to those of the undoped BiFeO$_3$, which may affect the magnetic structure in the doped samples (Table I).

Figure 3 shows field emission scanning electron microscope (FESEM) images of undoped and doped polycrystalline BiFeO$_3$ ceramics. FESEM image (Fig. 3(a)) of the BiFeO$_3$ pellet shows the presence of micro-grains with grain sizes of ∼10-20 μm. However, the grain sizes of the doped samples (Figs. 3(b) to 3(d)) were significantly reduced (∼400–500 nm). It is likely that Ca and Ba doping inhibits grain growth and furthers densification up to a certain level. As similar reduction in grain size was discussed in an earlier report on Pb doped BiFeO$_3$ ceramics.[22] Energy dispersive x-ray spectrum analysis of undoped and doped BiFeO$_3$ samples found a Bi: Fe ratio of approximately 1:1. The substitution of aliovalent ions (Ba^{2+} and Ca^{2+}) in the Bi^{3+} site of BiFeO$_3$ is expected to introduce oxygen vacancy defects.[17] The substitution of aliovalent A^{2+} ion at the Bi^{3+} site in Bi$_{0.9}$A$_{0.1-}$FeO$_3$ samples requires the appearance of oxygen vacancies in the host lattice, in accordance with the following defect chemistry model:[17]

$$0.45 Bi_2O_3 + 0.1 AO + 0.5 Fe_2O_3 \rightarrow Bi_{0.9}^{3+}A_{0.1}^{2+}Fe_1^{3+}O_{2.95}^{2+}$$
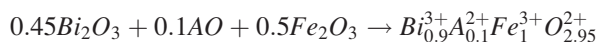
The charge imbalance introduced by the aliovalent doping is compensated by oxygen vacancies, which act as charge donors that may further increase the conductivity of these doped BiFeO$_3$ samples.

To identify the chemical bonding in these samples, we performed x-ray photoelectron spectroscopy (XPS) studies. The measured binding energies for Bi, Fe, and O confirmed the phase purity of the compounds. The XPS spectra for Fe are expanded from 700 to 740 eV in Fig. 4(a). The 3/2 and 1/2 spin–orbit doublet components of the Fe *2p* photoelectrons were located near 710.4 and 724.5 eV, respectively. The XPS result showed single-phase formation of BiFeO$_3$ (BFO), Bi$_{0.9}$Ca$_{0.1}$FeO$_{2.95}$ (BC10FO), Bi$_{0.9}$Ba$_{0.05-}$Ca$_{0.05}$FeO$_{2.95}$ (BB5C5FO), and Bi$_{0.9}$Ba$_{0.1}$FeO$_{2.95}$ (BB10FO) ceramic samples with a Fe^{3+} valence state. We do not find evidence for any Fe^{2+} impurities in the samples, which have previously been proposed as a source of enhanced electrical conductivity in other BiFeO$_3$ samples.[23] To explore the effect of doping on the oxygen state, we also measured the

O1s peaks in all samples and results are as shown in Fig. 4(b). There is a small shift in the binding energy of O1s peak of doped samples (530.7–531.6 eV) compared to that of undoped BiFeO$_3$ sample (530 eV). The oxygen absorption peak near 533.5 eV confirms the presence of oxygen vacancy defects in all doped BiFeO$_3$ samples. The formation of these oxygen vacancy defects may be attributed the aliovalent ion (Ba^{2+} and Ca^{2+}) substitution at Bi^{3+} ion of BiFeO$_3$ to maintain charge neutrality.[17]

We measured zero field cooled (ZFC) and field cooled (FC) magnetization curves for the BFO, BC10FO, BB5C5FO, and BB10FO samples at a magnetic field of 100 Oe in the temperature range, 2–320 K (Fig. 5). The ZFC and FC curves of undoped BiFeO$_3$ ceramics show an anomaly near 250 K, which marks a spin glass-like transition;[20,24] however, this anomaly was found to disappear in the Ba doped sample. The ZFC and FC curves for the BB10FO ceramic were found to overlap, suggesting the persistence of antiferromagnetic behavior down to 10 K. The ZFC and FC magnetization values of Ca doped BiFeO$_3$ (BC10FO) sample increased with decreasing temperature to 5 K and also yielded magnetization values an order of magnitude larger than that measured for the other samples indicating the presence of weak ferromagnetic ordering. However, the Ba-Ca co-doped BFO (BB5C5FO) sample also exhibited some weak ferromagnetic behavior
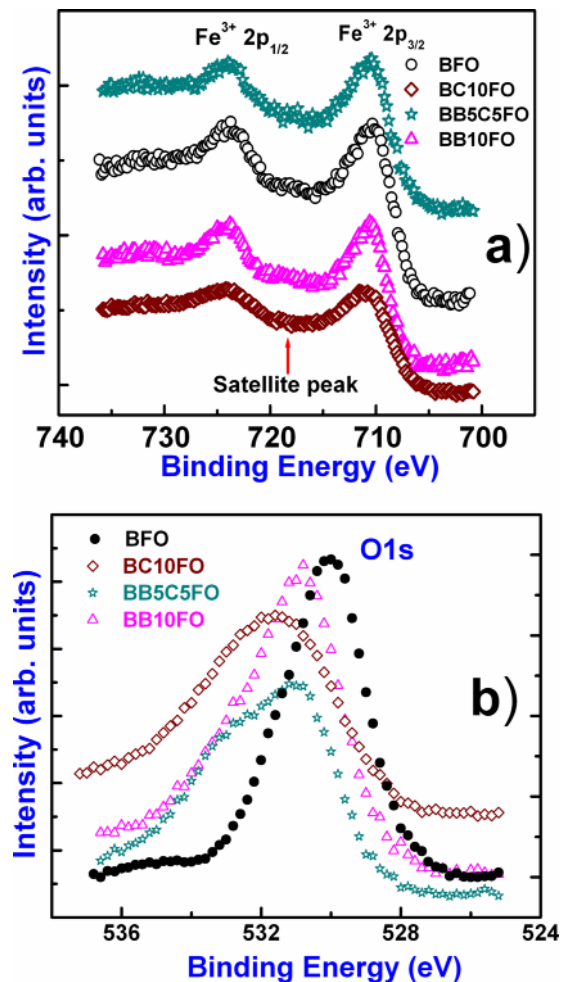

FIG. 4. (Color online) XPS spectra of (a) Fe element and (b) O1s of BFO, BC10FO, BB5C5FO, and BB10FO ceramics.
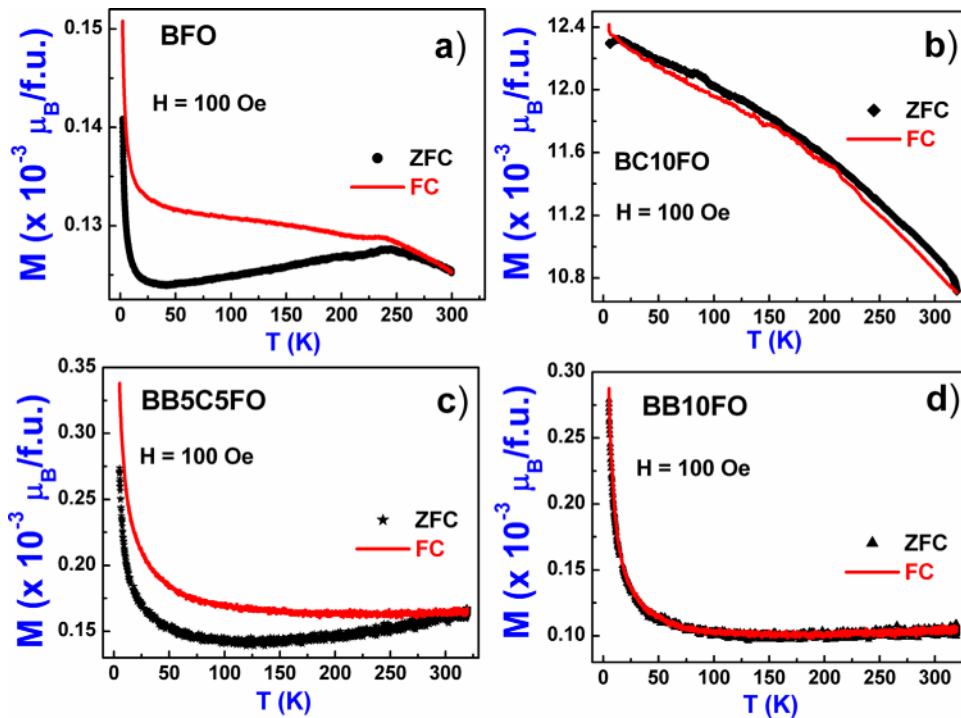
FIG. 5. (Color online) ZFC and FC magnetization of (a) BFO, (b) BC10FO, (c) BB5C5FO, and (d) BB10FO ceramics at a magnetic field of 100 Oe in the temperature range 2–320 K.

together with short range magnetic ordering, which is seen in ZFC and FC magnetization curves. Figure 6(a) plots the magnetization (M) versus magnetic field (H) for the BFO, BC10FO, BB5C5FO, and BB10FO samples measured at
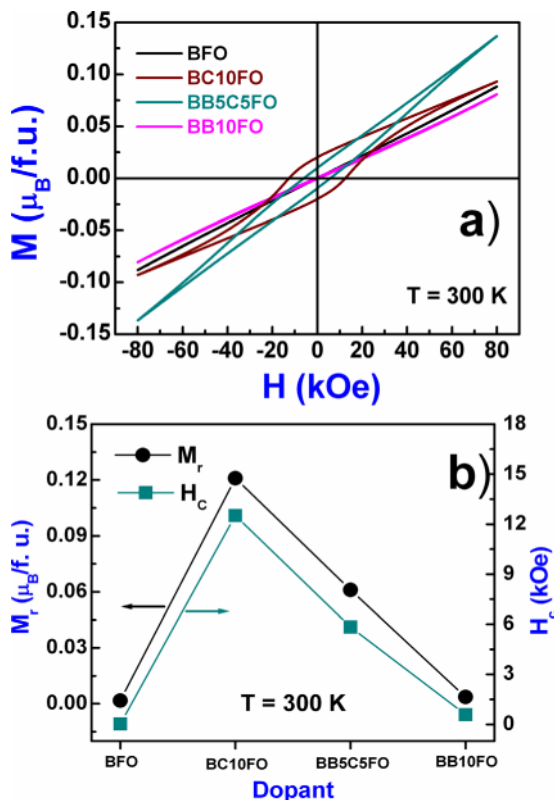

FIG. 6. (Color online) (a) Magnetization (M) vs magnetic field (H) curves of BFO, BC10FO, BB5C5FO, and BB10FO ceramics in a magnetic field of 80 kOe at 300 K and (b) Remnant magnetization (M_r) and coercive field (H_c) vs dopant.

300 K. The *M-H* curves of BC10FO and BB5C5FO samples showed weak ferromagnetic behavior at 300 K with no saturation even at an applied magnetic field of 80 kOe. Conversely, the *M-H* curves of BFO and BB10FO samples showed antiferromagnetic behavior at 300 K. From Fig. 6(b), we find that the remnant magnetization (M_r) of the BC10FO sample is about 0.12 μ_B/f.u. at 300 K; this is approximately 50 times larger than that of undoped BiFeO$_3$ (0.002 μ_B/f.u.). The coercive field (H_c) of BC10FO was also found to be very large (12.5 kOe at 300 K) compared to that of other three samples. However, Ba-Ca co-doped BiFeO$_3$ (BB5C5FO) showed moderate remnant magnetization (M_r) and coercive fields (H_c) of 0.06 μ_B/f.u. and 5.8 kOe at 300 K, respectively (Fig. 6(b)).

High-temperature zero field cooled (ZFC) magnetization measurements of polycrystalline BFO, BC10FO, BB5C5FO, and BB10FO ceramics were recorded using a vibrating sample magnetometer (model 74034 VSM, LakeShore, USA) at a magnetic field of 10 kOe in the temperature range 300–820 K (Fig. 7). We measured the high-temperature magnetization of undoped and doped BiFeO$_3$ samples to determine the antiferromagnetic transition temperatures (T_N) as well as to explore how the magnetic ordering is affected by Ba and Ca doping. The estimated antiferromagnetic transition temperatures (T_N) of BFO, BC10FO, BB5C5FO, and BB10FO samples were found to be 643 K, 647 K, 645 K, and 643 K, respectively. The transition is sharp in the Ca doped and Ba-Ca co-doped BiFeO$_3$ (BC10FO and BB5C5FO) samples. This may be associated with a sharp increase in paramagnetic susceptibility, which is an indication for weak ferromagnetism.[25] We also find that the transition temperature in Ca doped and Ba-Ca co-doped BiFeO$_3$ samples shifts to a higher temperature than that of the undoped BiFeO$_3$ sample. This may reflect the chemical pressure induced by Ca doping.[26]

These investigations provide a framework for improving the magnetic property of BiFeO$_3$ by divalent ion doping. A
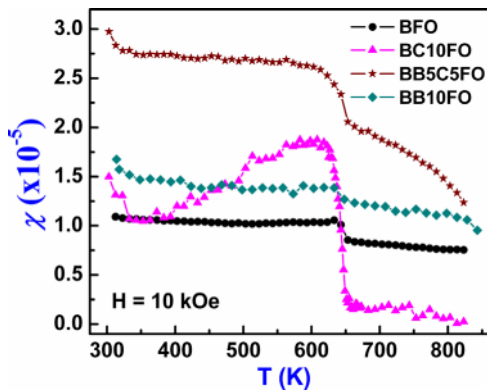
FIG. 7. (Color online) High-temperature dc magnetic susceptibility (χ-T) curves of BFO, BC10FO, BB5C5FO, and BB10FO ceramics recorded in a magnetic field of 10 kOe in the temperature range, 300–820 K.

weak ferromagnetic order can be induced in $BiFeO_3$ by chemical pressure produced by the replacement of Bi by smaller Ca^{2+} ions, which leads to contraction of the lattice, similar to the effects of hydrostatic pressure.[26] Substituting Ba into the lattice, which has a larger ionic size Bi leads to a reduction in grain size in the ceramic, producing better densification than for undoped $BiFeO_3$[22] and hence improving the ferroelectric properties of the polycrystalline sample (S).[27] However, the antagonistic effects of Ca and Ba doping on chemical pressure in this system means that the 1:1 co-doped samples do not have optimized physical properties. Significantly ameliorating the properties of $BiFeO_3$ ceramics by aliovalent doping on the A site will require tuning the chemical pressure to introduce weak ferromagnetic order, while simultaneously improving the sample density (S)[27] and reducing grain size.

IV. SUMMARY

Single-phase $BiFeO_3$, $Bi_{0.9}Ca_{0.1}FeO_{2.95}$, $Bi_{0.9}Ba_{0.05}Ca_{0.05}FeO_{2.95}$, and $Bi_{0.9}Ba_{0.1}FeO_{2.95}$ ceramic samples were synthesized using an ethanol mediated sol-gel approach. Structural refinement reveals that the samples have crystallized in rhombohedral structure with the non-centrosymmetric space group $R3c$. From SEM studies, the grain sizes of the doped samples were significantly reduced ($\sim$400–500 nm) compared to that of undoped $BiFeO_3$ (10–20 μm). XPS studies confirmed the formation of single-phase of $BiFeO_3$ ceramics with a Fe^{3+} valence state. Magnetic studies of the undoped and doped $BiFeO_3$ ceramic samples reveal Ca doped and Ba-Ca co-doped samples showed weak ferromagnetic behavior at room temperature. It is also found that the transition temperature in Ca doped and Ba-Ca co-doped $BiFeO_3$ samples shifts to higher temperatures, which is due to chemical pressure induced by Ca doping. These studies pinpoint Ca doped and Ba-Ca co-doped $BiFeO_3$ samples as interesting material systems for magnetoelectric coupling studies.

[1]M. Fiebig, J. Phys. D **38**, R123 (2005).
[2]W. Prellier, M. P. Singh, and P. Murugavel, J. Phys.: Condens. Matter **17**, R803 (2005).
[3]J. Wang, H. Zheng, Z. Ma, S. Prasertchoung, M. Wuttig, R. Droopad, J. Yu, K. Eisenbeiser, and R. Ramesh, Appl. Phys. Lett. **85**, 2574 (2004).
[4]W. Eerenstein, N.D. Mathur, and J. F. Scott, Nature, **442**, 759 (2006).
[5]S. W. Cheong and M. Mostovoy, Nat. Mater. **6**, 13 (2007).
[6]R. Ramesh and N.A. Spaldin, Nat. Mater. **6**, 21 (2007).
[7]M. Gajek, M. Bibes, S. Fusil, K. Bouzehouane, J. Fontcubert, A. Barthelemy, and A. Fert, Nat. Mater. **6**, 296 (2007).
[8]G. Srinivasan, E. T. Ramussen, and R. Hayes, Phys. Rev. B **67**, 014418 (2003).
[9]P. Fischer, M. Polomska, I. Sosnowska, and M. J. Szymański, Phys. C **13**, 1931 (1980).
[10]I. Sosnovska, M. Loevenhaupt, W. I. F. David, and R. M. Ibberson, Phys. B **180/181**, 117 (1992).
[11]J. Wang, J. B. Neaton, H. Zheng, V. Nagarajan, S. B. Ogale, B. Liu, D. Viehland, V. Vaithyanathan, V. D. G. Schlom, U. V. Waghmare, N. A. Spaldin, K. M. Rabe, M. Wuttig, and R. Ramesh, Science **299**, 1719 (2003).
[12]Y. P. Wang, L. Zhou, M. F. Zhang, X. Y. Chen, J.-M. Liu, and Z. G. Liu, Appl. Phys. Lett. **84**, 1731 (2004).
[13]M. M. Kumar, V. R. Palkar, K. Srinivas, and S. V. Suryanarayana, Appl. Phys. Lett. **76**, 2764 (2000).
[14]J. B. Neaton, C. Ederer, U. V. Waghmare, N. A. Spaldin, and K. M. Rabe, Phys. Rev. B **71**, 014113 (2005).
[15]V. R. Palkar, D. C. Kundaliya, S. K. Malik, and S. Bhattacharya, Phys. Rev. B **69**, 212102 (2004).
[16]R. K. Mishra, D. K. Pradhan, R. N. P. Choudhary, and A. Banerjee, J. Magn. Magn. Mater. **320**, 2602 (2008).
[17]V. A. Khomchenko, D. A. Kiselev, J. M. Vieira, L. Jian, A. L. Kholkin, A. M. L. Lopes, Y. G. Pogorelov, J. P. Araujo, and M. J. Maglione, J. Appl. Phys. **103**, 024105 (2008).
[18]B. Bhushan, A. Basumallick, S. K. Bandopadhyay, N. Y. Vasanthacharya, and D. Das, J. Phys. D **42**, 065004 (2009).
[19]C.-H. Yang, J. Seidel, S. Y. Kim, P. B. Rossen, P. Yu, M. Gajek, Y. H. Chu, L. W. Martin, M. B. Holcomb, Q. He, P. Maksymovych, N. Balke, S. V. Kalinin, A. P. Baddorf, S. R. Basu, M. L. Scullin, and R. Ramesh, Nat. Mater. **8**, 485 (2009).
[20]B. Ramachandran and M. S. Ramachandra Rao, Appl. Phys. Lett. **95**, 142505 (2009).
[21]A. C. Larson and R. B. Von Dreele, Los Alamos National Laboratory Report No. LAUR 86-748, 1994.
[22]R. Mazumder and A. Sen, J. Alloy. Compd. **475**, 577 (2009).
[23]X. Qi, J. Dho, R. Tomov, M. G. Blamire, and J. L. M. Driscoll, Appl. Phys. Lett. **86**, 062903 (2005).
[24]M. K. Singh, W. Prellier, M. P. Singh, R. S. Katiyar, and J. F. Scott, Phys. Rev. B **77**, 144403 (2008).
[25]T. Moriya, Phys. Rev. **120**, 91 (1960).
[26]G. Catalan, K. Sardar, N. S. Church, J. F. Scott, R. J. Harrison, and S. A. T. Redfern, Phys. Rev. B **79**, 212415 (2009).
[27]See supplementary materials at http://dx.doi.org/10.1063/1.3678449 for ferroelectric data.